Engineering Structures 24 (2002) 869–879

ENGINEERING STRUCTURES

www.elsevier.com/locate/engstruct

Performance of concrete structures retrofitted with fibre reinforced polymers

Shamim A. Sheikh *

Department of Civil Engineering, 35 St. George Street, University of Toronto, Toronto, Ontario, Canada M5S 1A4

Received 14 September 2001; received in revised form 6 December 2001; accepted 15 December 2001

Abstract

Retrofitting with fibre reinforced polymers (FRP) to strengthen and repair damaged structures is a relatively new technique. In an extensive research program underway at the University of Toronto, application of FRP in concrete structures is being investigated for its effectiveness in enhancing structural performance both in terms of strength and ductility. The structural components tested so far include slabs, beams, columns and bridge culverts. Research on columns has particularly focussed on improving their seismic resistance by confining them with FRP. All the specimens tested can be considered as full-scale to two-third scale models of the structural components generally used in practice. Results so far indicate that retrofitting with FRP offers an attractive alternative to the traditional techniques. In many circumstances, it can provide the most economical (and superior) solution for a structural rehabilitation problem. Selected results from experimental and analytical research are presented in this paper.

Keywords: Beams; Columns; Ductility; Fibre reinforced polymers (FRP); Repair; Retrofitting; Seismic; Slabs

1. Introduction

Repair and retrofitting of existing structures have become a major part of the construction activity in many countries. In large part, this can be attributed to aging of the infrastructure, and increased environmental awareness in societies. Some of the structures are damaged by environmental effects which include corrosion of steel, variations in temperature, freeze–thaw cycles and exposure to ultra-violet radiation. There are always cases of construction-related and design-related deficiencies that need correction. Many structures, on the other hand, need strengthening because the allowable loads have increased, or new codes have made the structures substandard. This last case applies mostly for seismic regions, where new standards are more comprehensive than the old ones.

Traditional retrofitting techniques that use steel and cementitious materials do not always offer the most appropriate solutions. Retrofitting with fibre reinforced polymers (FRP) may provide a more economical and technically superior alternative to the traditional techniques in many situations. The FRPs are lighter, more durable and have higher strength-to-weight ratios than traditional reinforcing materials such as steel, and can result in less labour-intensive and less equipment-intensive retrofitting work.

In this paper, the use of FRP for the retrofitting of beams, slabs, walls and columns is investigated. Tests on near full-size models of wall-slabs, beams and columns were carried out to evaluate the beneficial effects of using external FRP reinforcement. Wall-slab specimens were repaired to improve their flexural resistance, while beam specimens were retrofitted for shear enhancement [1]. These tests were inspired by the damage sustained by a two-year old multi-storey concrete structure. The column specimens were tested under simulated earthquake loads [2]. Although the extensive test program included a large number of specimens, the results from only a select group of different types of specimens are presented here, due to space limitations.

* Tel.: +1-416-978-3671; fax: +1-416-978-7046.
E-mail address: sheikh@civ.utoronto.ca (S.A. Sheikh).

0141-0296/02/$ - see front matter
PII: S0141-0296(02)00025-1

2. Experimental program

2.1. Specimens

Near full-scale models of wall-slab specimens, beams and columns were tested under realistic loads. The critical section in the wall-slab specimens was subjected to pure flexure, while the beam test was shear-critical. The column specimens were tested to evaluate the performance of the plastic hinge region under cyclic shear and flexure while simultaneously subjected to a constant axial load.

2.2. Wall-slab specimens

Each of the three wall-slab specimens was 250 mm thick, 1200 mm wide and 2100 mm long, and represented a full-scale model of a floor slab or a foundation wall (Fig. 1). Reinforcement in the direction of span consisted of 4–10M (100 mm^2) bottom bars and 3–10M top bars. Transverse reinforcement was provided by 5–10M top and bottom bars. Small steel plates (40×25 mm) were welded to the ends of the longitudinal bars to ensure anchorage. Each wall-slab specimen was instrumented with 15 electric strain gauges on the longitudinal bars. Since two of the three specimens were to be repaired with FRP, it was decided to grind the bottom surfaces to yield a smooth, clean surface to ensure good bond between the concrete and the FRP.

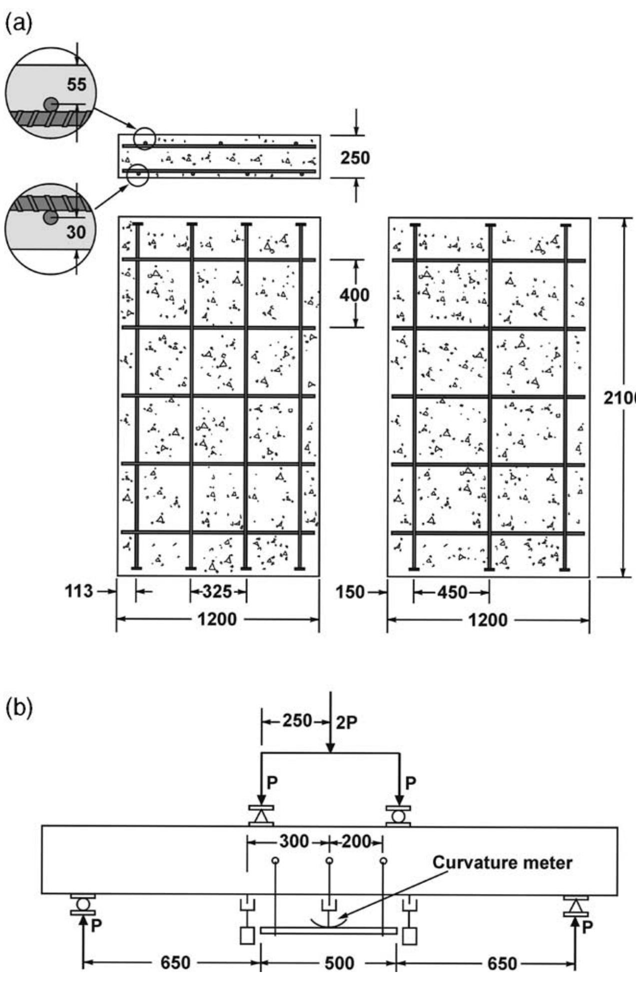

Fig. 1. Wall-slab specimen details and loading.

2.3. Beam specimens

Fig. 2 shows the dimensions and reinforcement details of the two beam specimens in which the test section was 1000 mm deep and 550 mm wide. Test loading is also shown in the figure. The beams in the actual building framed into walls. This was simulated by building a haunched region and increasing the amount of reinforcement for that half of the beam. As a result, shear failure was expected in the shallower part of the beam similar to that observed in the field. Each beam specimen contained 21 electric strain gauges on longitudinal and transverse steel. The casting was carried out in two steps. In the first step, the beam was cast without the haunch. Three days later, the haunch was constructed.

2.4. Column specimens

Each of the eight column specimens consisted of a 356 mm diameter and 1470 mm long column cast integrally with a 510×760×810 mm stub (Fig. 3). All columns were tested under lateral cyclic loading while simultaneously subjected to constant axial load throughout the test. Each column contained six 25M (500 mm^2) longitudinal steel bars, and the spirals were made of US#3 (71 mm^2) bars. The reinforcement for the stub consisted of 10M (100 mm^2) horizontal and vertical stirrups at 64 mm spacing. The design of the specimens aimed at ensuring that failure occurred in the potential plastic hinge region of the column (i.e. within a distance of 800 mm from the face of the stub), by reducing spiral pitch outside the test region. All the specimens were cast together in the vertical position.

The first group of column specimens consisted of steel-reinforced columns S-1NT, S-2NT, S-3NT and S-4NT. Specimens S-1NT and S-2NT contained the amount of spiral reinforcement which satisfied the ACI and Canadian code provisions [3,4] for seismic resistance, whereas specimens S-3NT and S-4NT contained much less spiral reinforcement. These four control columns were tested to failure to establish the standard behaviour against which columns retrofitted with FRP could be compared. The second group consisted of four columns ST-2NT to ST-5NT which contained the same amount of spiral reinforcement as specimens S-3NT and S-4NT, but were strengthened with GFRP or CFRP before testing. Each specimen had 18 strain gauges installed on longitudinal bars, and 6–9 strain gauges on the spiral. In addition, 24 linear variable differential

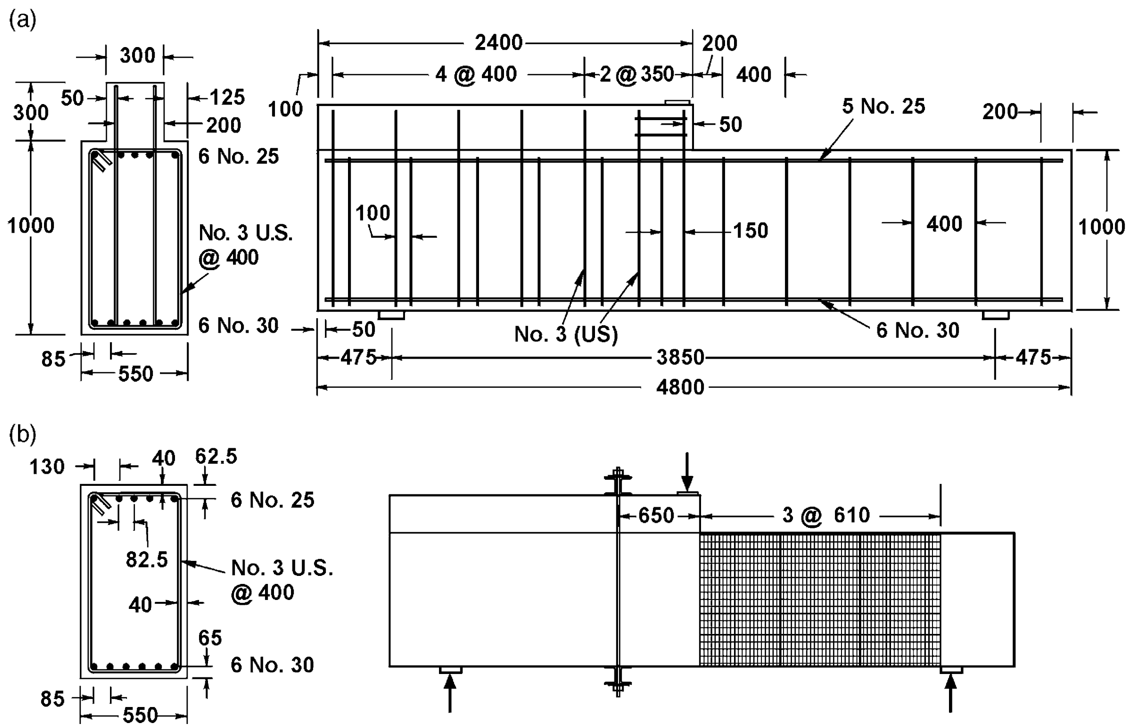

Fig. 2. Details of beam specimens. (a) Cross section and reinforcement details. (b) Zone of FRP-repair.

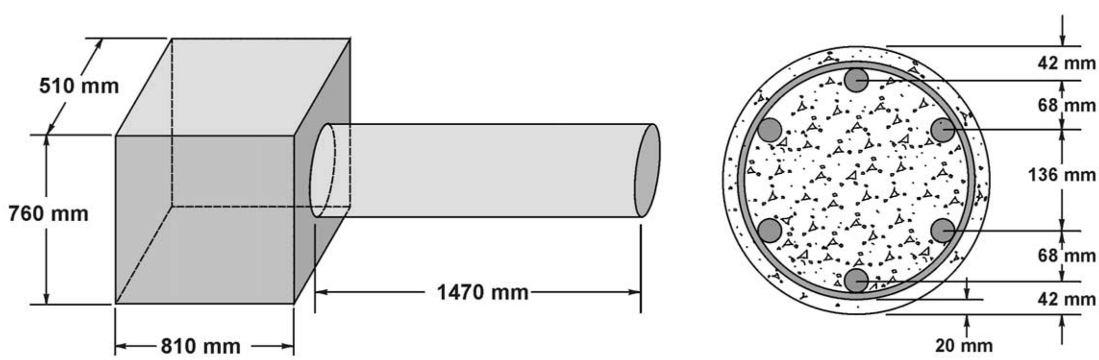

Fig. 3. Column specimen.

transducers (LVDTs) were used to measure deflection and deformation in the core of the columns.

2.5. Materials

TYFO FIBERWRAP system was used for retrofitting. The epoxy was prepared by mixing two components as suggested by the manufacturer. The carbon or glass fabric was saturated with the epoxy, and a layer of epoxy was also applied to the surface of the specimen. The saturated fabric was then applied to specimens, with fiber orientation in the appropriate direction. Fig. 4 shows a typical FRP test coupon and the tensile behaviour of the three types of FRP employed. Since the thickness of composite depends on the amount of epoxy used, strength is represented as a force per unit width instead of stress.

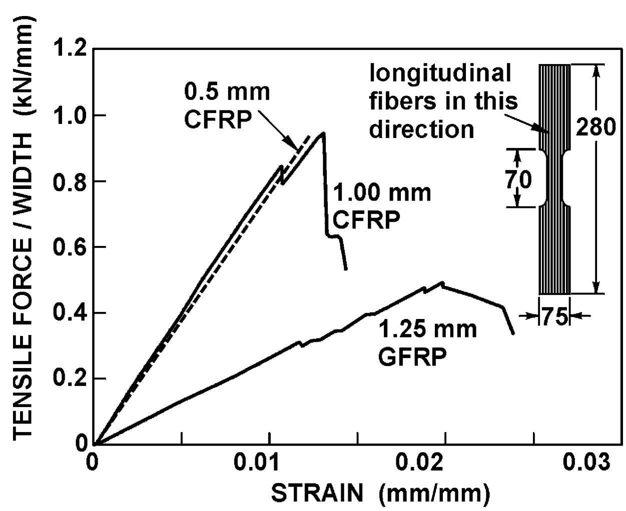

Fig. 4. Tensile characteristics of FRP.

Ready-mixed concrete, with specified compressive strength of 30 MPa and 20 mm maximum size coarse aggregate, was used. Development of concrete strength with age was monitored by testing two or three cylinders at one time. The strength of concrete in wall-slab specimens varied between 48.4 and 53.9 MPa, while in the two beam specimens it was 44.7 and 45.7 MPa. Cylinder strength for concrete in the columns ranged between 39 and 45 MPa.

Deformed bars were used in all the specimens. US #3 bars (71 mm^2) were of grade 60 steel, while grade 400 steel was used for Canadian sizes 10M (100 mm^2), 25M (500 mm^2) and 30M (700 mm^2). Fig. 5 shows the stress–strain curves for the steel bars used in the test program.

3. Testing

3.1. Wall-slab specimens

The three wall-slab specimens were tested under deformation control in a 2700-kN universal MTS testing machine (Fig. 6). Two line loads were applied to the specimens (simply supported at two ends) to produce flexural cracking similar to that observed in the field. Two curvature meters and three LVDTs were also used to measure deformations during loading, in addition to the strain gauges installed on the steel cages. The cracks (as they developed under load) were monitored in specimen Wall1 to determine the point at which the other two specimens (Wall2 and Wall3) would be repaired. Specimen Wall1 failed in flexure at a total load of 193 kN.

Specimen Wall2 was initially loaded to 135 kN. The average strain at the centre of the bottom flexural steel was 3.3×10^{-3} at this stage. Two flexural cracks had formed at this load. The crack widths at various locations varied between 0.3 and 0.7 mm at the bottom of the slab, with an average width of about 0.4 mm. These cracks were similar to the ones measured in the field. As a result, the displacement was maintained at this level while the repair was carried out with carbon FRP composite. All external instrumentation was removed in order to apply the fabric. Three strips of fabric approximately 600 mm in width were used, as shown in Fig. 7. The outer strips of fabric were folded and bonded to the sides of the specimen to eliminate premature FRP separation from the concrete. In the field, sufficient anchorage length was available to develop the full strength of the FRP. The epoxy was allowed to cure for three days, during which the load fell to about 115 kN

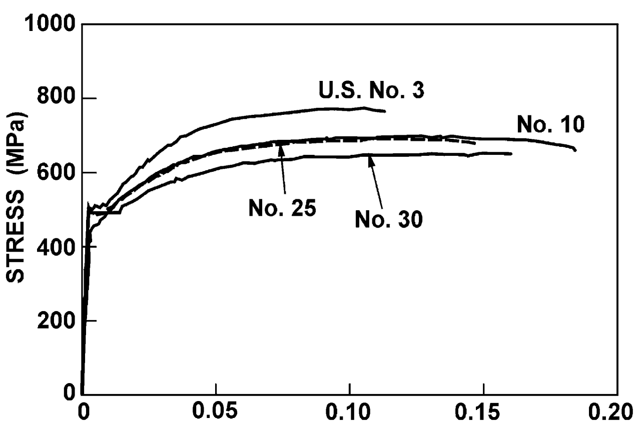

Fig. 5. Stress–strain characteristics of steel.

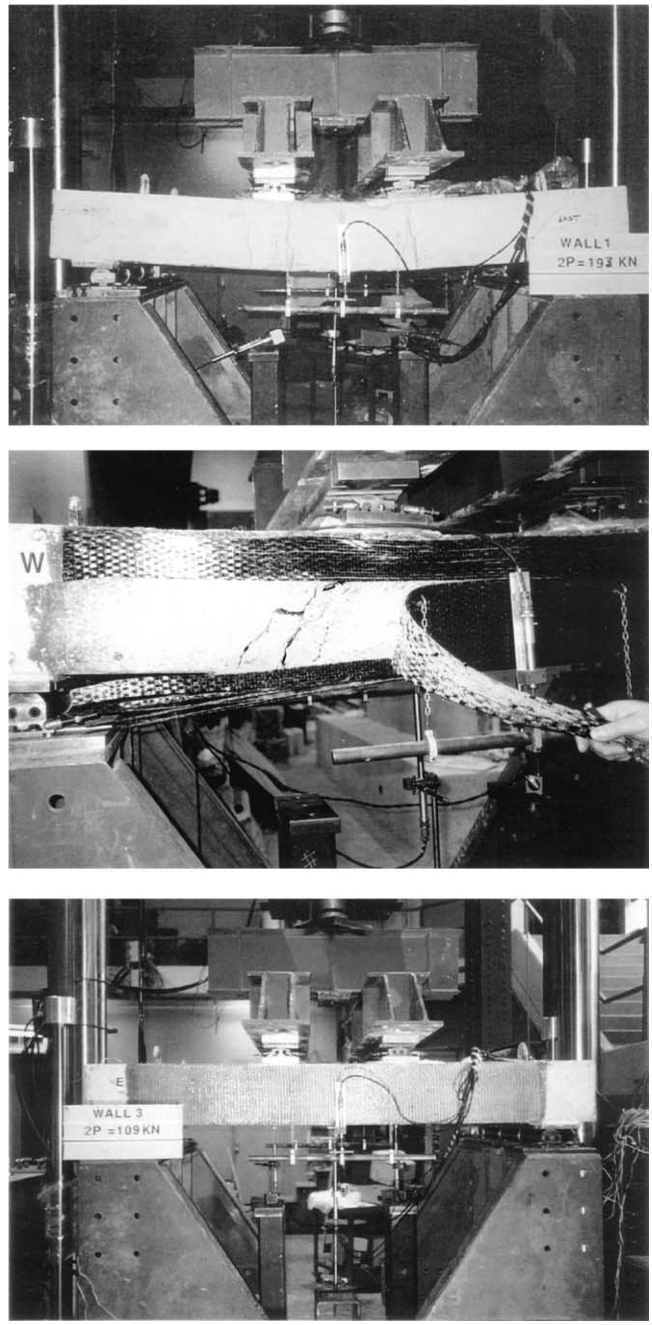

Fig. 6. Wall-slab specimens 1, 2 and 3.

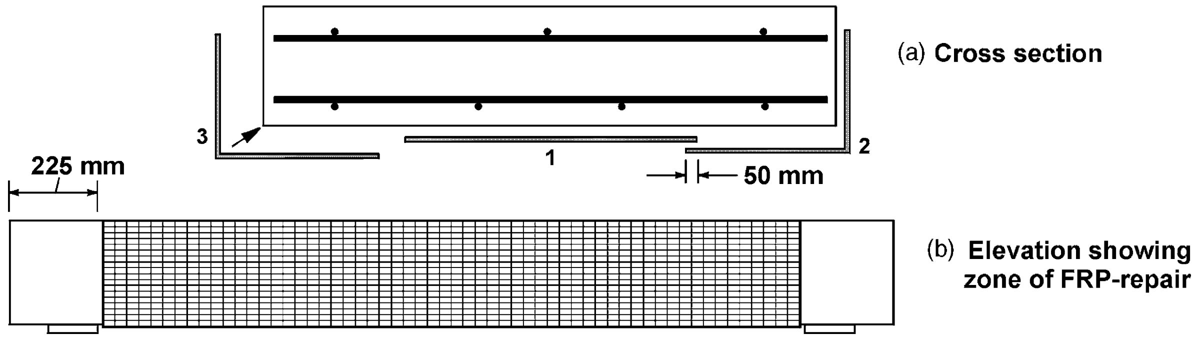

Fig. 7. Details of FRP retrofitting of wall-slab specimens.

under constant displacement. At the end of this time, the external instrumentation was re-applied and the load was increased until the specimen failed in shear at a load of 478 kN, with large inclined cracks and delamination of the CFRP.

The third specimen (Wall3) was tested the same way as specimen Wall2, except that glass FRP was used for repair. The behaviour of specimen Wall3 was similar to that of Wall2, but shear failure occurred at an applied load of 422 kN.

3.2. Beam specimens

A single point load was applied on the haunched portion to test the beam and produce cracking similar to that encountered in the field. External instrumentation consisting of linear variable differential transducers was used to obtain information about the shear strain and the deflection profile as the test progressed.

The first specimen, Beam1, was considered as a control specimen against which the performance of the FRP-retrofitted beam was to be measured. Fig. 8 shows the tested Beam1. As the load was increased, several shear cracks appeared and were monitored to determine the similarity of distress between the specimen and the beams in the building. At a load of 1600 kN, crack widths exceeded 2.0 mm; the beam failed in a brittle manner at a load of 1700 kN, corresponding to a deflection of 14 mm. This mode of failure is typical of large beams that are shear-critical and contain very light shear reinforcement.

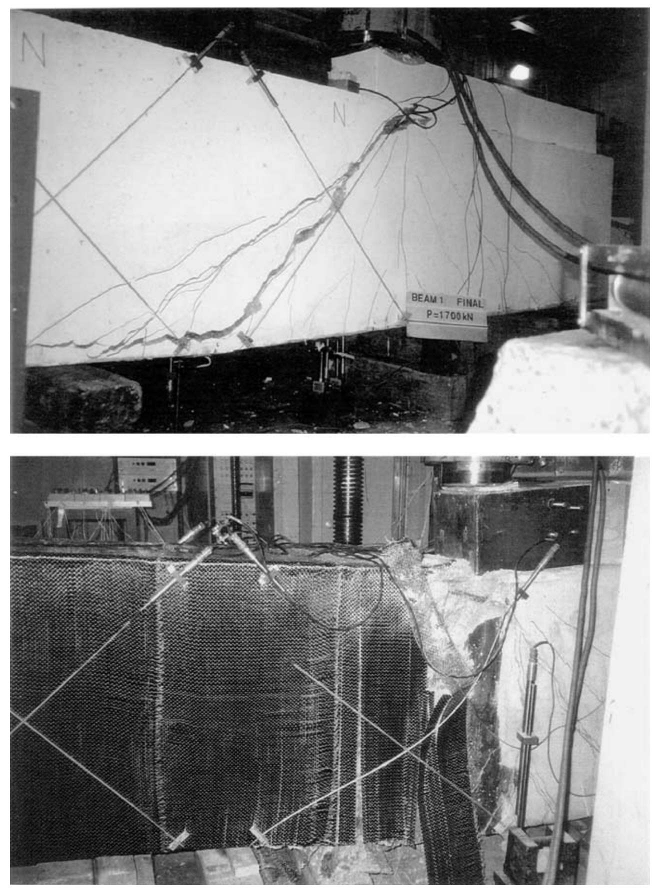

Fig. 8. Specimens beam 1 and 2 at failure.

The specimen Beam2 was loaded to 1180 kN when five diagonal cracks, ranging in width from 0.2 to 0.8 mm, were observed. The average tensile strain at the centre of the bottom flexural steel was approximately 1.5×10^{-3} at this stage. The crack pattern and the crack widths appeared similar to what was observed in the beams of the building. As a result, the displacement imposed on the beam was maintained while the repair procedure was initiated by removing all the external instrumentation. Three strips of fabric, each approximately 610 mm in width, were wrapped around the specimen in the damaged zone (Fig. 2). The specimen remained under load for three days for the duration of repair and curing of epoxy. The load during this time dropped from 1180 kN to approximately 1000 kN. After re-installing the instrumentation at the end of this time, the loading was re-commenced. The specimen was unloaded a few times to either readjust various instruments to capture large deformations, or to strengthen the haunched portion of the beam under the load point (which showed signs of concrete failing). The maximum load reached in this beam was 2528 kN, corresponding to a deflection of 143 mm. The final failure was caused by the rupture of carbon fabric at a top edge close to the applied load as shown in Fig. 8. Before the repair was carried out, the sharpness of the edges was somewhat reduced by slight grinding. A well-rounded edge perhaps would have eliminated this type of CFRP rupture.

3.3. Column specimens

The test setup is shown in Fig. 9. A hydraulic jack with a capacity of 4450 kN was used to apply the axial load, and the cyclic lateral load was applied by an MTS actuator having 1000-kN load capacity and ±150 mm stroke capacity. Prior to testing, each specimen was aligned both vertically and horizontally, until the centreline of the column coincided with the line of action of the axial load. All the specimens were subjected to cyclic lateral displacement while simultaneously carrying a constant axial load throughout the test. The lateral load sequence, shown in Fig. 10, consisted of one cycle to a displacement of $0.75\Delta_1$, followed by two cycles each to Δ_1, $2\Delta_1$, $3\Delta_1$ and so on, until the specimen was unable to maintain the applied axial load. The deflection parameter Δ_1 was defined as the lateral deflection corresponding to the maximum lateral load along a line that represented the initial stiffness of the specimen, as illustrated in Fig. 10.

In all the ‘S’ series column specimens (Group I), the most extensive damage was concentrated in the column at about 295–350 mm from the stub face. During the last cycle, buckling of longitudinal bars was observed, which indicated the commencement of failure. Spiral steel fractured in specimens S-1NT and S-2NT, and brought about the termination of the tests. However, in specimens S-3NT and S-4NT, spiral reinforcement did not yield. For the ‘ST’ series specimens, separation of fabric from concrete along the circumference was observed within the hinging zone, as indicated by a change in FRP color, during the fourth or fifth cycle when the concrete crushed. As the applied displacement increased, this separation of the FRP wraps extended for a distance of 200–400 mm from the stub.

During the wrapping of the FRP, the fabric was weakened by the extruded LVDT bars, which could cause premature rupture of the composite. To avoid this type of failure, one additional FRP strip of 75 mm width was installed along the extruded LVDT bars on all the specimens reported here. The most extensive damage for all the columns with FRP wraps occurred at about 250–300 mm from the stub face, which is also the location of the first fiber rupture. Failure for all specimens was dominated by flexural effects. No cracking was observed in the stub in any specimen.

4. Results and discussion

4.1. Wall-slabs

The load vs maximum-deflection curves for the three specimens are presented in Fig. 11. Although the use of

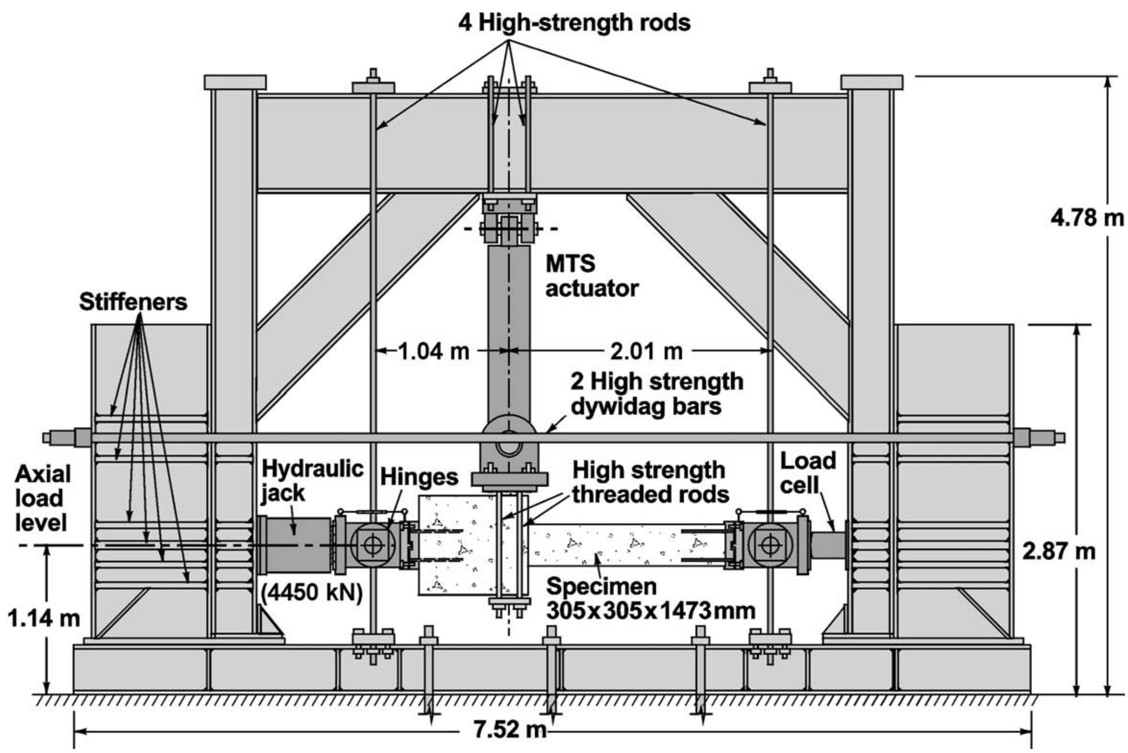

Fig. 9. Test setup for columns.

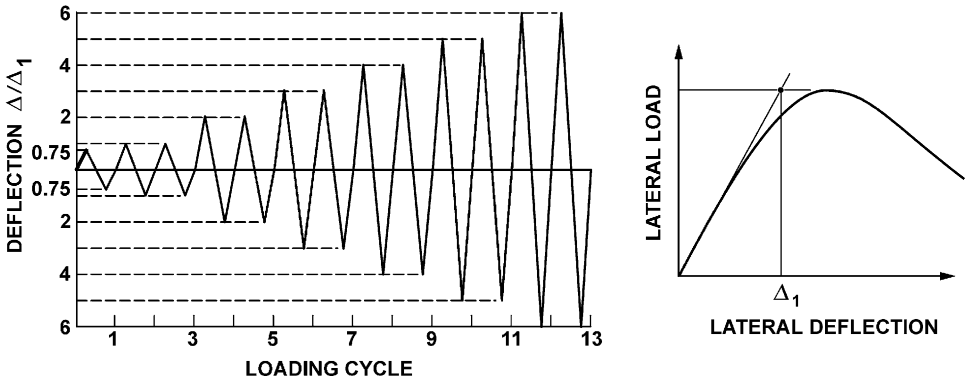

Fig. 10. Specified displacement history.

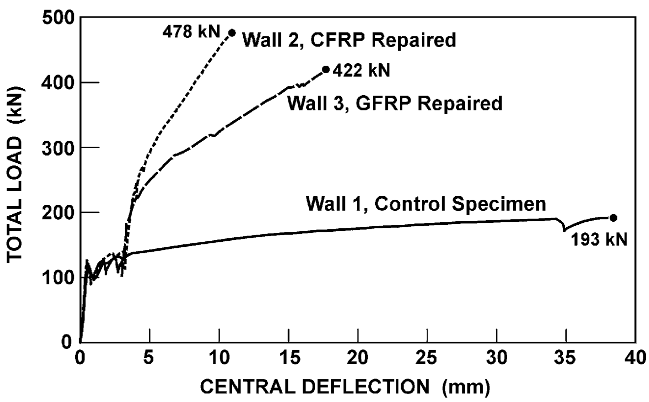

Fig. 11. Load–deflection behaviour of wall-slab specimens.

FRP resulted in a substantial (119% for GFRP and 148% for CFRP) increase in the ultimate capacity of the slabs, the full potential of FRP was not realized in the repaired slabs. The external FRP reinforcement was aimed at maximizing the enhancement in the flexural capacity of the slabs without causing premature bond failure of FRP or its peeling off the concrete surface. The load corresponding to the shear capacity was much lower than that for the enhanced flexural capacity. The failure in both repaired slabs was, therefore, caused by shear.

From the available analytical procedures, the moment–curvature responses of the three wall-slab specimens were developed. In addition to hand calculations, a computer program RESPONSE developed at the University of Toronto by Bentz [5], was also used to calculate the response. For Wall1, hand calculations were performed without tension stiffening effects as well as with a tension-stiffening factor of 0.5. As shown in Fig. 12, the yield and the ultimate moment capacities are better predicted by ignoring the tension stiffening factor. Program RESPONSE automatically adjusts for the effect of tension stiffening, based on the information provided.

In the repaired specimens, the initial curvature at the time of repair was considered in the analysis by allowing for the initial strains in the slab section. The analytical moment–curvature curves from RESPONSE shown in Fig. 12 simulate the experimental behaviour reasonably well up to the point when both specimens failed in shear. The analytical curves are shown up to a point where a quick drop in load was observed. Table 1 shows the experimental and analytical failure loads and moment values. For Wall1, the analytical moment capacity was determined by hand calculations using the code provisions [3,4]. The analytical values for repaired specimens Wall2 and Wall3 are based on the shear capacity calculated according to the general method of the Canadian Code [4].

4.2. Beams

The load–deflection curves for the two beams are shown in Fig. 13. Whereas Beam1 failed in shear at a load of 1700 kN, Beam2 retrofitted with CFRP had an ultimate capacity of 2528 kN and failed in flexure. The maximum deflection at failure in the original beam was 14 mm under the load point, which increased to 143 mm in the repaired beam. The energy dissipation capacity of the repaired beam was more than 2600% of that of the original beam. The failure load for the control beam, based on the shear capacity calculated from the Canadian Code [3], was 1095 kN for the General Method and 1167 kN for the Simplified Method. The beam capacity calculated from the ACI Code [1] equations is 1561 kN. Load estimates from both codes were conservative. The shear span–depth ratio of the beam was approximately equal to 2.0, which may have contributed to the development of compression struts after significant cracking had occurred (and hence to the larger shear capacity observed in the test).

In the application of code equations to predict the shear capacity of the repaired beam, the carbon fabric was considered as a series of equivalent stirrups. The shear failure load based on the General Method of the Canadian Code [3] was 5245 kN. The shear capacity from the ACI Code [1] and the Simplified Method of the Canadian Code [3] was 4985 kN. The beam, however, failed in flexure at a load of 2528 kN. The analyti-

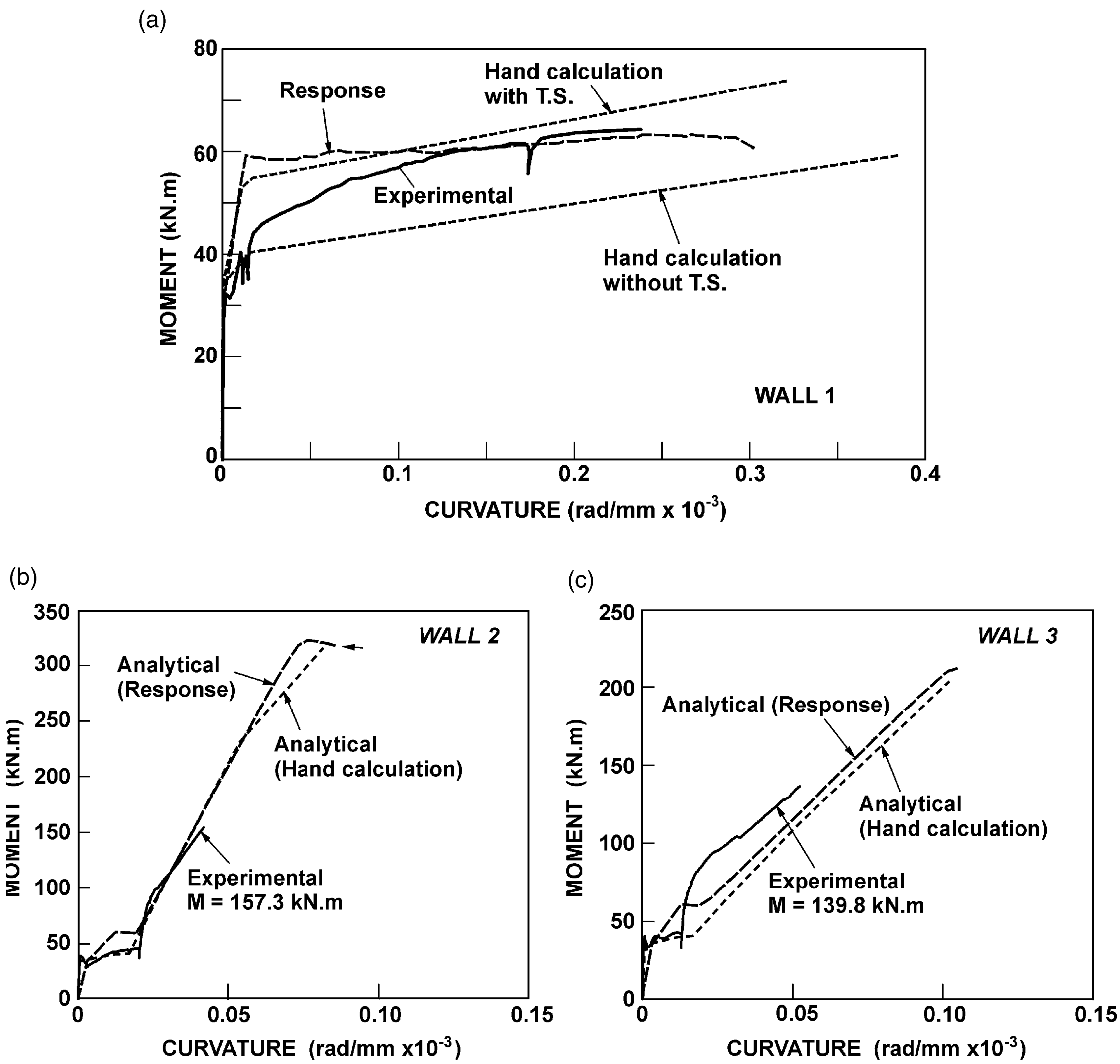

Fig. 12. Experimental and analytical moment curvature responses for wall-slab specimens.

Table 1
Load and moment values at failure in wall-slab specimens

Specimen	Experimental		Analytical		Failure mode
	Load (kN)	Moment (KN-m)	Load (kN)	Moment (KN-m)	
WALL1	193	62.7	182	59.1	Flexure
WALL2	478	155.4	484	157.3	Shear
WALL3	422	137.2	430	139.8	Shear

cal moment–curvature response of the beam section subjected to the maximum moment is shown in Fig. 14 along with the behaviour obtained from the test. The two curves agree quite well. It should be noted that the analytical flexural response in Fig. 14 is unaffected by the presence of FRP.

4.3. Columns

The column section adjacent to the stub was subjected to the maximum moment, but failure in all the columns initiated at a location 200–400 mm away from the stub. A few representative column failures are shown in Fig.

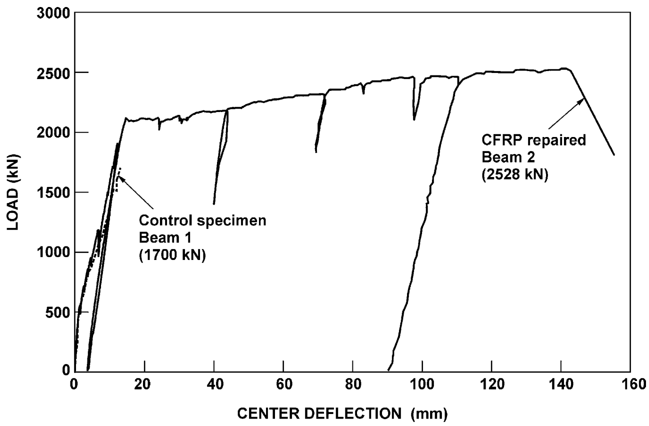

Fig. 13. Load–deflection behaviour of beam specimens.

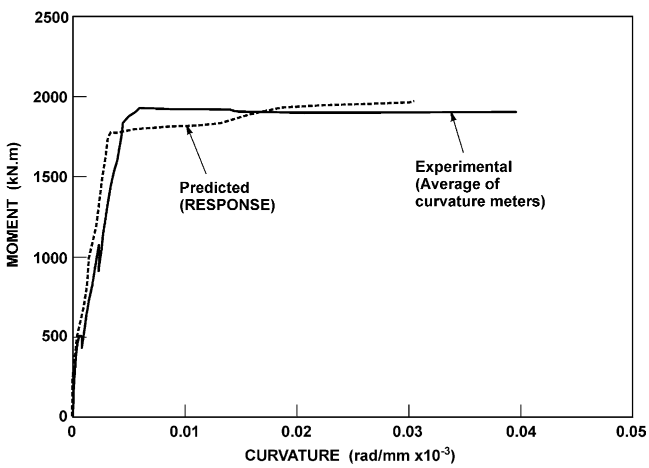

Fig. 14. Comparison of predicted and measured responses of repaired beam.

15. The additional confinement provided by the stub strengthened the critical section, such that failure took place at a location of lesser moment away from the stub. The moment–curvature responses of the most damaged column sections are presented in Fig. 16 for the eight columns. A number of variables can be examined by comparing different specimens.

An increase in axial load from $0.27P_o$ in specimen S-2NT to $0.54P_o$ in specimen S-1NT resulted in reduced ductility and deformability of the column. The energy dissipation capacity of the section under lower axial load is approximately seven times that of the section under high axial load. It should be noted that columns in specimens S-1NT and S-2NT were designed according to seismic provisions of the ACI and Canadian Codes [3,4]. Although the test results show that the amount of confining reinforcement should be larger for higher axial loads in columns, the required amount of confining reinforcement is not a function of the level of axial load in these codes. The effect of the amount and spacing of spiral reinforcement can be examined by comparing the behaviour of specimen S-1NT with that of S-3NT, and the behaviour of S-2NT with that of S-4NT. An increase in the amount of spiral reinforcement provides higher confining pressure, and the reduced spiral pitch improves the stability of the longitudinal bars, thus resulting in more ductile behaviour of the columns. Energy dissipation capacity of the columns with more spiral reinforcement and reduced pitch is orders of magnitude larger than that of specimens with smaller amount of spiral steel placed with larger pitch.

The effectiveness of FRP in strengthening deficient columns can be evaluated by considering two sets of specimens. The first set includes specimens S-1NT, S-3NT, ST-2NT and ST-3NT tested under an axial load of $0.54P_o$. Specimen S-3NT was similar to specimens ST-2NT and ST-3NT in all respects, except the lack of FRP. Comparison of the behaviour of these three specimens shows the remarkable beneficial effects of FRP wrapping on strength and ductility of columns. While S-3NT failed during the fifth load cycle (maximum displacement of $3\Delta_1$), specimens ST-2NT and ST-3NT, retrofitted with two layers of GFRP and one layer of CFRP respectively, were able to sustain 12 load cycles with a maximum displacement of $6\Delta_1$ and 11 load cycles with a maximum displacement of $5\Delta_1$, respectively. Both the retrofitted specimens showed no strength degradation. Energy dissipation capacity of the critical sections of the columns increased by a factor of about 40 due to retrofitting with GFRP and CFRP. Behaviour of the two FRP-strengthened specimens was even better than that of specimen S-1NT, in which the spiral reinforcement satisfied the seismic code provisions of the ACI and Canadian Codes [3,4].

The second set of columns which were tested under $P=0.27P_o$ includes specimens S-2NT, S-4NT, ST-4NT and ST-5NT. Specimen S-4NT was identical to specimens ST-4NT and ST-5NT in all respects, except the lack of FRP. Similar to the first set, specimens strengthened with FRP displayed higher energy dissipation capacity and strength than specimen S-4NT. The overall responses of specimens ST-4NT and ST-5NT, retrofitted with FRP, were similar to or better than that of specimen S-2NT in which the spiral reinforcement was designed according to the seismic code provisions of the codes [3,4]. Under an axial load of $0.27P_o$, one layer of carbon or glass FRP increased the energy dissipation capacity of the section by a factor of more than 100.

From a comparison of specimens ST-3NT and ST-4NT, it can be seen that the amount of confinement required to produce comparably ductile behaviour of columns depends on the level of axial load. Both columns were confined to a similar degree with CFRP reinforcement, but the column under larger axial load displayed considerably less ductile behaviour. A similar conclusion can also be drawn from a comparison of specimens ST-2NT and ST-5NT. A two-fold increase in axial load

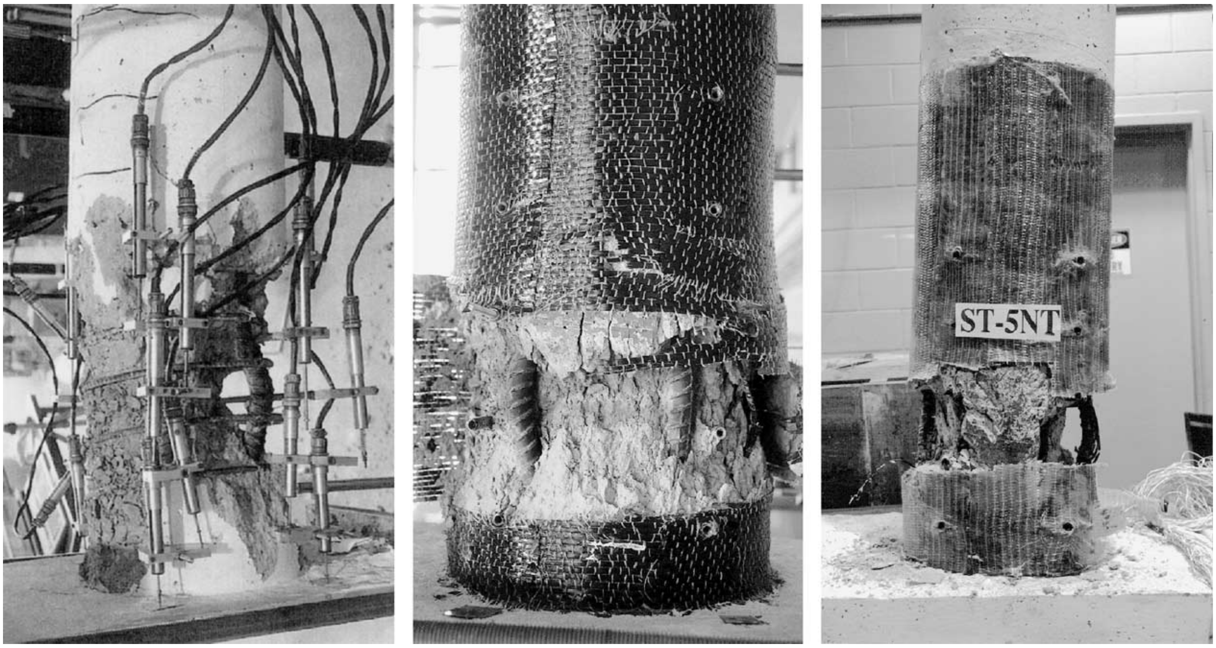

Fig. 15. Column specimens S-2NT, ST-3NT and ST-5NT after testing.

appears to require more than twice the amount of lateral FRP reinforcement for a comparable improvement in a column's ductile performance.

The results clearly indicate that a column designed and detailed for non-seismic response can be upgraded with relative ease with FRP wraps to match or exceed the performance of columns designed according to seismic provisions of the codes [3,4].

5. Concluding remarks

Results from testing of slab, beam and column specimens have been presented. Responses of specimens retrofitted with FRP are compared with those of the specimens without FRP. It is concluded that retrofitting with FRP provides a feasible rehabilitation technique for repair as well as strengthening. FRP reinforcing was very effective in enhancing flexural strength of the damaged slabs, shear resistance of the damaged beams and seismic resistance of columns.

Both carbon and glass composites provided significant enhancement (approximately 150%) in flexural strength, to the extent that failure of wall-slab specimens shifted to the shear mode. The shear mode of failure may not be acceptable in many cases. Caution is therefore required to limit the increase in flexural capacity due to FRP reinforcement. Wrapping of the large-size beam with one layer of CFRP changed the brittle mode of shear failure at 1700 kN to a very ductile flexural failure at 2528 kN. Available analytical techniques, including code equations, were found to provide reasonable estimates of the capacities for the retrofitted specimens.

Use of carbon and glass wraps improved the seismic resistance of columns in a very significant manner. Behaviour of FRP-confined columns under simulated earthquake loads matched or exceeded the performance of columns designed according to seismic provisions of the North American codes. Under an axial load approximately equal to the sections' balanced load, one layer of CFRP or GFRP enhanced the column's energy dissipation capacity by over 100 times. Columns designed with typical non-seismic details can therefore be upgraded economically with relative ease. FRP reinforcement required under an axial load of $0.54P_o$ was slightly more than twice that needed for an axial load of $0.27P_o$ for similar performance enhancement.

Acknowledgements

The experimental work reported here was conducted with the financial assistance of the Natural Sciences and Engineering Research Council (NSERC) under strategic grant no. STR 195771 and a grant from ISIS, an NSERC Network of Centres of Excellence. The tests were conducted in the Structures Laboratories at the University of Toronto. Technical and financial assistance from R.J. Watson Inc. of East Amherst, NY, Fyfe Co. of San Diego, CA, and RoadSavers Central Ltd of Toronto is gratefully acknowledged.

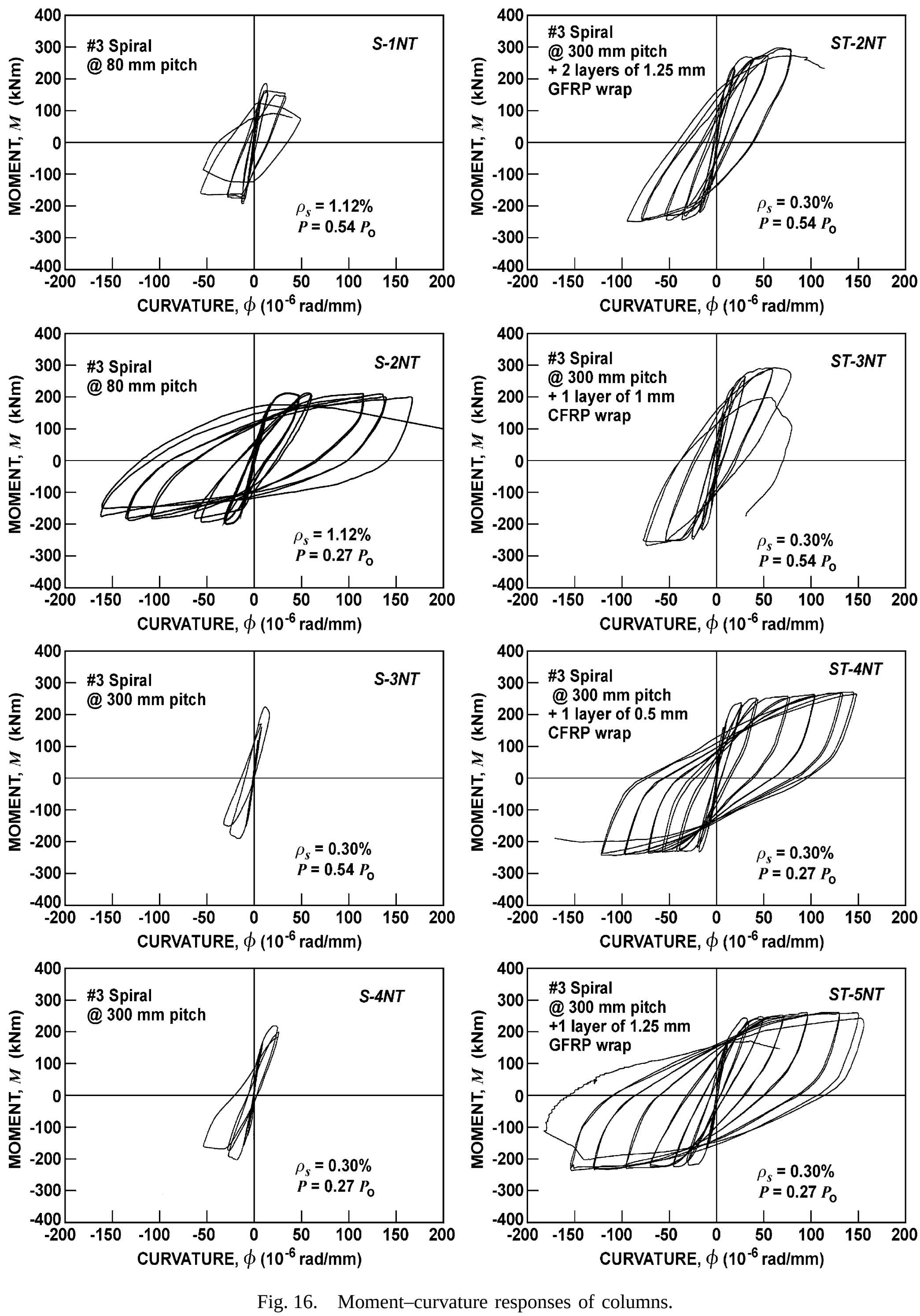

Fig. 16. Moment–curvature responses of columns.

References

[1] DeRose D, Sheikh SA. Rehabilitation of a concrete structure using fibre-reinforced plastics. Research report, Department of Civil Engineering, University of Toronto, Toronto, Canada; 1997. 170 pp.

[2] Yau G, Sheikh SA. Repair and strengthening of columns with fibre reinforced composites. Research report, Department of Civil Engineering, University of Toronto, Toronto, Canada; 1998. 199 pp.

[3] ACI Committee 318. Building code requirements for reinforced concrete and commentary (ACI 318-99/ACI 318R-99). American Concrete Institute, Detroit; 1999. 391 pp.

[4] Canadian Standards Association. Code for the design of concrete structures (A23.3-1994). Rexdale, Ontario, Canada; 1994. 199 pp.

[5] Bentz E. Sectional analysis of reinforced concrete members. PhD thesis, Department of Civil Engineering, University of Toronto, Toronto, Canada; 2000. 310 pp.